

A P2P-dominant Distribution System Architecture

Jip Kim, *Student Member, IEEE*, Matthew Roveto, *Student Member, IEEE*, and Yury Dvorkin, *Member, IEEE*

Abstract—Peer-to-peer interactions between small-scale energy resources exploit distribution network infrastructure as an electricity carrier, but remain financially unaccountable to electric power utilities. This status-quo raises multiple challenges. First, peer-to-peer energy trading reduces the portion of electricity supplied to end-customers by utilities and their revenue streams. Second, utilities must ensure that peer-to-peer transactions comply with distribution network limits. This paper proposes a peer-to-peer energy trading architecture, in two configurations, that couples peer-to-peer interactions and distribution network operations. The first configuration assumes that these interactions are settled by the utility in a centralized manner, while the second one is peer-centric and does not involve the utility. Both configurations use distribution locational marginal prices to compute network usage charges that peers must pay to the utility for using the distribution network.

NOMENCLATURE

A. Sets and Indices

| | |
|---|---|
| $b \in \mathcal{B}$ | Set of buses |
| $l \in \mathcal{L}$ | Set of distribution lines |
| $n \in \mathcal{N}$ | Sets of peers where $\mathcal{N}^{b/s}$ denote sets of buying/selling peers, $\mathcal{N}^b \cup \mathcal{N}^s = \mathcal{N}$ |
| $\omega \in \Omega$ | Set of peer trades |
| $\omega \in \Omega_n$ | Sets of trades of peer n , $\bigcup_{n \in \mathcal{N}} \Omega_n = \Omega$ |
| $\omega \in \Omega^*$ | Set of the matched peer trades, $\Omega^* \subseteq \Omega$ |
| $\Lambda_\omega = \{\rho_\omega^b, \rho_\omega^s\}$ | Set of buying/selling prices of trade ω |
| $b(\omega)/s(\omega)$ | Indices of buying/selling peers in trade ω |
| $o(l)/r(l)$ | Indices of originating/receiving-end nodes of distribution line l |

B. Parameters

| | |
|--------------------------------------|---|
| B_b | Susceptance of bus b [p.u.] |
| $C_n(\cdot)$ | Cost function of selling peer n [\$/MWh] |
| C_b^u | Cost of utility generator at bus b [\$/MWh] |
| C^w | Wholesale market electricity price [\$/MWh] |
| D_b^p/D_b^q | Active/reactive power demand [MW/MVA _r] |
| $\underline{D}_n^p/\overline{D}_n^p$ | Minimum/maximum power bought by peer n [MW] |
| G_b | Conductance of bus b [p.u.] |
| $\underline{G}_n^p/\overline{G}_n^p$ | Minimum/maximum power sold by peer n [MW] |
| P | Standard trade size [MW] |
| $\underline{P}_b^g/\overline{P}_b^g$ | Minimum/maximum real power output limit of utility generator at bus b [MW] |
| $\underline{Q}_b^g/\overline{Q}_b^g$ | Minimum/maximum reactive power output limit of utility generator at bus b [MVA _r] |
| R_l | Resistance of distribution line l [p.u.] |
| S_l | Apparent flow limit of distribution line l [MVA] |
| T_b | Electricity tariff at bus b [\$/MWh] |
| $U_n(\cdot)$ | Utility function of buying peer n [\$/MWh] |
| $\underline{V}_b/\overline{V}_b$ | Minimum/maximum limit on the squared voltage magnitude at bus b |
| X_l | Reactance of distribution line l [p.u.] |
| Γ_b | Penetration level of the peer trading at bus b |
| Π^u | Revenue of the power utility [\\$] |
| Υ_n | Value of electricity surplus for peer n [\$/MW] |
| $\Delta\rho$ | Value of adjustment in price |

C. Variables

| | |
|--------------|--|
| a_l | Squared current flow of distribution line l |
| c_ω^n | Network usage charge for trade ω [\$/MWh] |

| | |
|-------------------------------|---|
| d_n^p | Power bought by peer n [MW] |
| f_l^p/f_l^q | Active/reactive power flow of distribution line l [MW/MVA _r] |
| g_n^p | Power sold by peer n [MW] |
| p_b^g/q_b^g | Active/reactive power output of utility generator at bus b [MW/MVA _r] |
| p_ω | Power transfer from $s(\omega)$ to $b(\omega)$ in trade ω [MW] |
| v_b | Squared nodal voltage magnitude of bus b |
| η_l^+/ η_l^- | Dual variable of forward/backward flow limit constraints on distribution line l |
| λ_b | Dual variable of the active power balance constraint at bus b |
| μ_b | Dual variable of the reactive power balance constraint at bus b |
| $\rho_\omega^b/\rho_\omega^s$ | Buying/selling price of trade ω [\$/MWh] |

I. INTRODUCTION

Owing to recent advances in smart grid technologies, the U.S. power grid is undergoing nation-wide modernization. One of the most important objectives of this modernization is to achieve a high degree of supply autonomy of electricity consumers from their local electric power utility and the freedom to choose their electricity suppliers. In practice, the supply autonomy and the freedom to choose are enabled by rolling out customer-end distributed energy resources (DERs), which include, but not limited to, photovoltaic panels, battery energy storage, and demand-side management. If these DERs are appropriately sized and operated, electricity consumers are shown to significantly reduce, if not completely eliminate, their dependency on the electricity supply from the utility.

While the roll-out of DERs offers significant reliability and economic benefits to both the utility and consumers, it reduces revenue streams of the utility and undermines their financial viability. Furthermore, accommodating large-scale DER deployment also imposes technical challenges on the distribution network operations since the current electric power distribution infrastructure was not designed to deal with bidirectional power flows, increased voltage fluctuations and volatile nodal power injections induced by DERs. As a response to these challenges, utilities in many U.S. regions have already started increasing electricity tariffs, thus further incentivizing remaining consumers to adopt DERs and exacerbating their impact on the distribution system [1]. This self-fueling process – colloquially known as the utility’s death spiral – calls for urgent changes to the current electric power distribution practice. Accordingly, 94% of the senior power and the utility executives surveyed by PricewaterhouseCoopers predict ‘complete transformation [...] to the power utility business model’ by 2030, [2].

These techno-economic challenges observed by utilities motivate to re-think and re-engineer interactions between stand-alone DERs and utilities to continue harvesting their benefits without compromising supply reliability. Among possible alternatives, the peer-to-peer (P2P) architecture is regarded as a viable coordination mechanism that can efficiently operate heterogeneous DERs, [3], while respecting physical limits

on the distribution network. The P2P architecture assumes a less centralized, more autonomous and flexible electricity delivery, in which small-scale (e.g. residential and commercial) producers and consumers can transact electricity and other services as an alternative to centralized electricity supply from utilities or third-party aggregators.

Unlike the current distribution practice that mainly pursues the economies of scale and scope benefits [4], the value proposition of the P2P architecture stems from the sharing economy [5]. The sharing economy monetizes under-utilized or otherwise suboptimally used resources due to the failure of utilities and aggregators to effectively communicate with and aggregate DERs, [4], [6]. However, the current regulatory environment does not incentivize power utilities to accommodate P2P, thus hindering their value to the system [4], [7].

The literature on P2P interactions in distribution systems is thin and still emerging. Morstyn *et al.* [8]–[10] leverage the concept of full substitutability [11], i.e. an equilibrium condition for peers in a hierarchical supply chain, to develop a bilateral contract network for P2P energy trading. This contract network allows for forward (e.g. day-ahead) and real-time energy trading that produce a time-static, network-unconstrained stable equilibrium that peers have no incentive to deviate from. Park *et al.* [12] derived a closed form of network-unconstrained Nash equilibrium among peers in microgrids and Tushar *et al.* [13] review game- and auction-theoretic approaches to represent the P2P interactions under different implementation scenarios. Relative to [11], [12], the authors of [13] generalize the definition of the P2P equilibrium in the network-constrained context. While [13] emphasizes the importance of accounting for network constraints in P2P transactions, it does not describe how it can be done. To account for possible network limitations, Ahn *et al.* [14] restrict P2P interactions to neighboring nodes and exploit the Lagrangian duality to compute the electricity and “energy flow” prices. The latter price is used to charge peers for using the network infrastructure operated by utilities, but does not capture the effect of P2P interactions in other (more remote) distribution grid locations. This limitation is partly addressed by Baroche *et al.* [15], where the authors consider P2P energy transactions across a given network and account for basic power flow constraints via the DC power flow approximation. The model in [15] can also enforce a fixed, exogenous charge on peers for using the utility’s network infrastructure. However, the use of the DC approximation does not reflect the distribution network physics (e.g. losses, voltage regulation, reactive power support) and, thus, the actual cost incurred by the utility. Furthermore, exogenously set charges in [15] do not capture spatio-temporal dynamics of the distribution system and sensitivities of peers. Münsing *et al.* [16] present a blockchain-enabled decentralized P2P market-clearing algorithm using a convexified AC optimal power flow (OPF) and exploit the distribution locational marginal prices (DLMPs) to settle transactions among peers. Building on [16], Wang *et al.* [17], [18] leverage blockchains to design a “Crowdsourced energy system” with a P2P energy trading for day-ahead and real-time operations. Although [16]–[18] incentivize P2P interactions, they do not compensate the power utilities for peers’ usage of the distribution network.

The P2P matching mechanisms, i.e. methods to connect peering producers and consumers, can be classified as either system-centric [13]–[18] or peer-centric [8]–[10], [12]. The

system-centric matching resembles pool-structured wholesale electricity markets with the single supervisory entity that collects and matches the bids and offers submitted by market participants in a centralized manner. On the other hand, the peer-centric approach is decentralized, which offers more flexibility for accommodating their preferences, [11], and allows for distributed decision-making protocols that preserve privacy of peers, [19], [20]. Regardless of the matching mechanism chosen, the large-scale implementation of P2P interactions is expected to affect the ability of the utility to operate the distribution network efficiently and reliably.

This paper aims to construe a new electric power distribution architecture that will allow for a large volume of P2P interactions among small-scale DERs and shift electric power utilities from the current volumetric business model, when the revenue is proportional to the amount of electricity sold to customers, to a service-based business model, where the revenue is collected from providing services to support electricity trading by other parties. To this end, we conceptualize the P2P platform¹, i.e. a marketplace for direct energy transactions among peers, that can internalize both the system- and peer-centric matching approaches. To effectively accommodate P2P in the distribution system, the P2P platform is then integrated with a distribution AC OPF. This integration aims to capture the sharing economy benefits, without compromising supply reliability, and ensures that P2P interactions are accounted for in OPF-based energy management tools. Unlike [16]–[18], this paper uses the OPF framework to derive and compute network usage charges to be paid by peers for using the distribution network based on the DLMPs, [21]. The use of the DLMPs makes it possible to represent spatio-temporal dimensions of operating conditions in the distribution network and consider them while computing the network usage charges. In turn, the network usage charges are then used to encourage those P2P transactions that improve the overall distribution system performance and generate an additional revenue stream intended to offset the drop in the utility’s revenue caused by the roll-out of customer-end DERs.

II. DISTRIBUTION SYSTEM WITH THE P2P PLATFORM

Regardless of the peer matching mechanism chosen, it is important to consider generic interfaces that relates the P2P platform and the rest of the distribution system. Fig. 1 illustrates these interfaces for different volumes of the electricity supplied by the P2P platform as compared to the current distribution system architecture.

A. Current distribution system architecture

The current distribution system architecture is shown in Fig. 1(a), where the sole utility operates the distribution network, supplies electricity to customers and collects the electricity payment. Under this practice, the electricity prices for small-scale consumers are based on flat or time-of-use volumetric electricity rates. This rate is typically regulated and set to recover both the operating and capital costs incurred by the utility. The operating cost includes the cost of electricity supply, maintenance, network losses and control, while the capital cost includes the cost of expansion and upgrade projects. In this case, the revenue of the utility is:

¹Our definition of the P2P platform is technology agnostic, e.g. it can be enabled by either blockchains [12], [16]–[18] or other decentralized technologies.

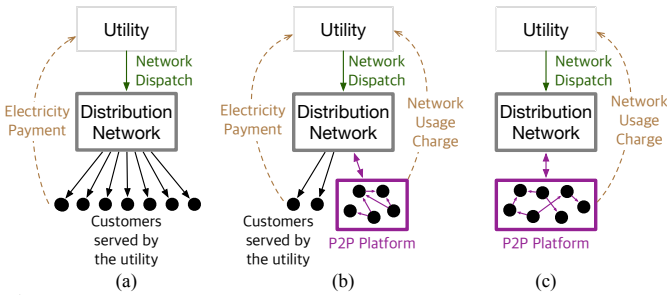


Fig. 1: Comparison of the distribution system architecture with and without the proposed P2P platform: (a) Current architecture, (b) Mixed architecture, (c) P2P architecture. Solid and dashed arrows represent energy and financial flows respectively.

$$\Pi^u = \sum_{b \in \mathcal{B}} T_b D_b^p \quad (1)$$

and is proportional to rate T_b and active power demand D_b^p , thus assuming all operating and capital costs are uniformly allocated among customers based on their electricity consumption. However, this approach fails to adequately capture the costs incurred by the customers that deployed their own DERs, which reduce or eliminate their electricity consumption provided by the utility and thus the utility revenue. Since rate T_b lumps together different operating and capital costs, it is impossible to accurately itemize the effect of DERs on the operating cost. Therefore, the current practice impedes further proliferation of DERs because it does not provide sufficient compensation for network services provided by the utility.

B. Distribution system architecture with the P2P platform

To overcome the limitations of the current practice, there is a trend to devise such rates that would itemize the effect of individual consumers and producers on distribution network operations. Recently, multiple studies [21], [22] proposed to introduce so-called DLMPs to separate the cost of electricity supply and various services related to the operation of the distribution network (e.g. power losses, voltage control, reactive power support). As in the unbundling of the transmission level, this separation aims to provide open access to the distribution network for third-party electricity providers (e.g. DER aggregators or stand-alone DERs) and to fairly charge them for using the distribution network.

Based on the open access assumption, we envision two possible distribution architectures that can replace the current architecture in Fig. 1(a). The mixed architecture illustrated in Fig. 1(b) preserves the current option of receiving electricity supply from the utility for some consumers and also enables the P2P interactions among stand-alone DERs and consumers. Under the mixed architecture, the P2P platform matches producing and consuming peers and sets the electricity price for them. Since the P2P transactions will rely on the utility to operate the network, the peers are also additionally charged by the utility for using the network infrastructure. Therefore, the utility revenue is given as follows:

$$\Pi^u = \sum_{b \in \mathcal{B}} T_b D_b^p (1 - \Gamma_b) + NUC(c_\omega^n, p_\omega), \quad (2)$$

where the first term represents the electricity payment from the customers that receive their electricity supply directly from the utility and $NUC(\cdot)$ is the total network usage charges collected by the utility from the peers participating in the P2P interactions. In Eq. (2), parameter $\Gamma_b \in [0, 1]$ defines the ratio

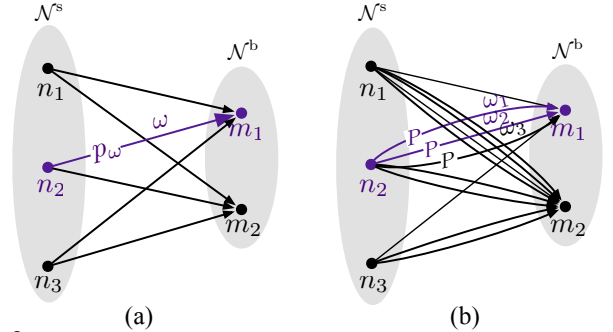


Fig. 2: A schematic representation of the peer matching process as (a) a simple bipartite graph for the system-centric configuration and (b) a bipartite graph with parallel edges for the peer-centric configuration. The edge represents trade ω of power p_ω between seller $s(\omega)$ and consumer $b(\omega)$.

between the total demand of a peer located at bus b served by the utility and by the P2P platform. Thus, the total demand procured by the P2P platform is $\sum_{\omega \in \Omega^*} p_\omega = \sum_{b \in \mathcal{B}} D_b^p \Gamma_b$.

The P2P architecture in Fig. 1(c) represents a particular case of the mixed architecture in Fig. 1(b), where the utility does not supply electricity and only supports network operations and the P2P platform satisfies the demand of all customers. In this case the utility revenue can be obtained by setting $\Gamma_b = 1$:

$$\Pi^u = NUC(c_\omega^n, p_\omega). \quad (3)$$

The key component of both the mixed and P2P architectures described above is network usage charge $NUC(c_\omega^n, p_\omega)$ that needs to be designed to recover the cost incurred by the utility while operating the distribution network and factored in the price formation process within the P2P platform.

III. P2P TRADING WITH NETWORK USAGE CHARGE

Implementing the P2P architecture, as shown in Fig. 1(b)-(c), requires routines to enable the peer matching process and to couple the P2P interactions with distribution network operations. Section III-A describes two distinct peer-matching routines, while Sections III-B and III-C introduce network usage charges to integrate these routines in one decision-making process with distribution network operations.

A. Peer matching process

We develop the peer-matching routines for two possible configurations that may arise in the future. The first configuration, referred to as system-centric, assumes that the utility will be responsible for matching the peers in a welfare-maximizing manner. By contrast, the peer-centric routine is carried out autonomously from the utility and is driven by preferences and choices of the peers.

For simplicity, both the system- and peer-centric configurations described below are developed under the assumption that a given peer can be either a producer or consumer, i.e. simultaneously producing and consuming is prohibited. Also, there are no exogenous restrictions on the set of possible matches between the consuming and producing peers. Under these two assumptions, the peer matching process in both configurations can be represented as a bipartite graph in Fig. 2. Each P2P energy trade ω is represented as an edge with sending and receiving nodes $n \in \mathcal{N}^s$ and $m \in \mathcal{N}^b$, respectively. We also denote node n of edge ω as seller $s(\omega) = n$ and node m as buyer $b(\omega) = m$ for every trade ω with the traded power denoted as p_ω . The system-centric configuration is

represented as a simple (trivial) bipartite graph in Fig. 2(a), i.e. there is only one edge (trade) connecting a buying and a selling peer. Therefore, the number of potential matches to be considered is $|\Omega| = \text{card}(\mathcal{N}^s) \times \text{card}(\mathcal{N}^b)$, and the objective of the matching process is to determine power transfer p_ω between peers given in trade set Ω . On the other hand in the peer-centric configuration that allows peers to negotiate trade prices, all trades have standard size $p_\omega = P$ and there can be multiple trades between a buyer and a seller to satisfy their needs. Therefore, the peer-centric configuration is represented as a bipartite graph with multiple parallel edges in Fig. 2(b), where edges $\omega_1, \omega_2, \omega_3$ denote multiple trades of the standard size). The number of parallel edges between seller n and buyer m is calculated as $\min\{\bar{G}_n^p/P, \bar{D}_m^p/P\}$ where \bar{G}_n^p and \bar{D}_m^p are the generation capacity of seller n and the maximum demand of buyer m . Then the number of potential matches to be considered is $|\Omega| = \sum_{n \in \mathcal{N}^s, m \in \mathcal{N}^b} \min\{\bar{G}_n^p/P, \bar{D}_m^p/P\}$.

1) *System-centric configuration*: The system-centric configuration is modeled as follows:

$$\max_{\Xi^{\text{P2P}}} O^{\text{P2P}} := \left(\sum_{n \in \mathcal{N}^b} U_n(d_n^p) - \sum_{n \in \mathcal{N}^s} C_n(g_n^p) \right) \quad (4a)$$

$$\underline{G}_n^p \leq g_n^p \leq \bar{G}_n^p, \quad \forall n \in \mathcal{N}^s, \quad (4b)$$

$$\underline{D}_n^p \leq d_n^p \leq \bar{D}_n^p, \quad \forall n \in \mathcal{N}^b, \quad (4c)$$

$$g_n^p = \sum_{\omega \in \Omega_n} p_\omega, \quad \forall n \in \mathcal{N}^s, \quad (4d)$$

$$d_n^p = \sum_{\omega \in \Omega_n} p_\omega, \quad \forall n \in \mathcal{N}^b, \quad (4e)$$

$$p_\omega \geq 0 \quad \forall \omega \in \Omega. \quad (4f)$$

where $\Xi^{\text{P2P}} = \{g_n^p, d_n^p, p_\omega, \geq 0\}$. The objective function in Eq. (4a) optimizes the welfare of all peers by maximizing the difference between the utility functions of consumers (U_n) and cost functions of producers (C_n). Eq. (4b) imposes limits on the power that can be sold based on the physical limits of producer $n \in \mathcal{N}^s$. Similarly, the Eq. (4c) establishes the minimum and maximum limits on the power purchased by buyer $n \in \mathcal{N}^b$. Note that Eq. (4c) models elastic consumers that can adjust their consumption based on their utility function. However, if the consumers are inelastic, Eq. (4c) can be converted into an equality by setting $\underline{D}_n^p = \bar{D}_n^p$. Eq. (4d) sets the total power sold by producer $n \in \mathcal{N}^s$ and Eq. (4e) computes the total power received by consumer $n \in \mathcal{N}^b$ from all producers, where Ω_n defines the trade set for peer n :

$$\Omega_n = \begin{cases} \{\omega \in \Omega | s(\omega) = n\}, & \text{if } n \in \mathcal{N}^s, \\ \{\omega \in \Omega | b(\omega) = n\}, & \text{if } n \in \mathcal{N}^b. \end{cases} \quad (5)$$

Eq. (4f) sets the power transfer from a seller to a buyer to non-negative values. The outcome of the optimization in Eq. (4) yields set of optimal matches Ω^* . The system-centric optimization in Eq. (4) pursues the system-wide welfare-maximization at the expense of sacrificing preferences of individual peers (e.g. cost minimization for consumers or profit maximization for producers) that may act strategically in order to increase their individual welfare. Therefore, the optimization in Eq. (4) reminisces wholesale pool electricity markets.

2) *Peer-centric configuration*: Unlike the system-centric optimization in Eq. (4), the peer-centric configuration matches the peers with respect to preferences of individual peers. This

process is decentralized and, therefore, can be carried out independently from the utility. As a result, each peer has the capability to negotiate, accept and reject trade ω based on their preferences, including bounded rationality and privacy considerations [23], [24]. The objective of the negotiation process is to establish a stable match between producers and consumers, i.e. there is no incentive to deviate from the cleared transactions unless the availability of producers or demand of consumers change. To obtain a stable match, we leverage the recent result by Morstyn *et al.* [8] that exploits the concept of full substitutability [11], which ensures that a decentralized price-adjustment process can be performed based on local information available to the peers and only requires communication between the peers engaged in trade ω . Since the peer-centric configuration requires no central coordinator (e.g. the utility in the system-centric configuration), it does not necessarily achieve a welfare-maximizing solution.

The stable match for each peer can be obtained as, [8]:

$$\Omega_n^* = \begin{cases} \arg \max_{\Omega_n} \{ \sum_{\omega \in \Omega_n} \rho_\omega^s p_\omega - C_n(g_n^p) \}, & \forall n \in \mathcal{N}^s, \\ \arg \max_{\Omega_n} \{ U_n(d_n^p) - \sum_{\omega \in \Omega_n} \rho_\omega^b p_\omega \}, & \forall n \in \mathcal{N}^b, \end{cases} \quad (6a)$$

where:

$$U_n(d_n^p) = \begin{cases} \Upsilon_n(d_n^p - \underline{D}_n^p), & \text{if } d_n^p \geq \underline{D}_n^p \\ -\infty, & \text{otherwise} \end{cases}, \quad \forall n \in \mathcal{N}^b, \quad (6b)$$

$$g_n^p = \sum_{\omega \in \Omega_n} p_\omega, \quad \forall n \in \mathcal{N}^s, \quad (6c)$$

$$d_n^p = \sum_{\omega \in \Omega_n} p_\omega, \quad \forall n \in \mathcal{N}^b. \quad (6d)$$

Eq. (6a) is the objective function of buying/selling peer n that aims to select those trades $\Omega_n^* \subseteq \Omega$ which are optimal with respect to their preferences, where ρ_ω^b and ρ_ω^s are the buying and selling prices of trade ω . Eq. (6b) is the utility function of consumer n that factors in the elasticity of consumers and their willingness to adjust their consumption. The total power generation and demand of peer n are calculated in Eq. (6c) and (6d) as the sum of traded power p_ω over transactions $\omega \in \Omega_n$.

Based on the policy in Eq. (6), the stable match among all peers is achieved using the price adjustment process given in Algorithm 1, which is an iterative procedure that seeks consensus among all peers [8]. First, the buyer and the seller prices are initialized at zero for all trades in set Ω , and saved in set of trade prices Λ_ω . At the beginning of each iteration, trade price set Λ_ω is saved as $\Lambda_\omega^{\text{old}}$ and each peer construct their preferred trade set Ω_n^* by solving Eq. (6). Then for all trades that accepted by buyers but rejected by sellers, price ρ_ω^s or ρ_ω^b is adjusted by value $\Delta\rho$. If trade ω is selected by both seller $s(\omega)$ and buyer $b(\omega)$, then the current price is set as trade price ($\rho_\omega = \rho_\omega^s = \rho_\omega^b$). The adjustment process repeats until prices for all trades converge. Once all trades are settled, the collection of such trades is returned as set Ω^* .

B. Network usage charges

Although the peer-matching configurations presented in Section III-A stably generate the set of selected trades Ω^* , the matching outcomes are not guaranteed to comply with distribution network limits and, therefore, it may lead to overloading the distribution system assets. To avoid this overloading, the peer-matching process must consider network constraints. This can be accomplished by introducing network usage charges

Algorithm 1 Price Adjustment Process

```

1: initialization:
2: for  $\omega \in \Omega$  do  $\rho_\omega^b, \rho_\omega^s \leftarrow 0$ 
3:  $\Lambda_\omega := \{\rho_\omega^b, \rho_\omega^s\}, \quad \forall \omega \in \Omega$ 
4: adjustment:
5: do
6:    $\Lambda_\omega^{\text{old}} \leftarrow \Lambda_\omega, \quad \forall \omega \in \Omega$ 
7:   for  $n \in \mathcal{N}^s$  do
8:      $\Omega_n^* \leftarrow \arg \max_{\Omega_n} \{\sum_{\omega \in \Omega_n} \rho_\omega^s p_\omega - C_n(g_n^p)\}$ 
9:   for  $n \in \mathcal{N}^b$  do
10:     $\Omega_n^* \leftarrow \arg \max_{\Omega_n} \{U_n(d_n^p) - \sum_{\omega \in \Omega_n} \rho_\omega^b p_\omega\}$ 
11:   for  $\omega \in \Omega$  do
12:     if  $\omega \in \Omega_{b(\omega)}^*$  and  $\omega \in \Omega_{s(\omega)} \setminus \Omega_{s(\omega)}^*$  then
13:       if  $\rho_\omega^b > \rho_\omega^s$  then
14:          $\rho_\omega^s \leftarrow \rho_\omega^s + \Delta\rho$ 
15:       else
16:          $\rho_\omega^b \leftarrow \rho_\omega^b + \Delta\rho$ 
17:   while  $\Lambda_\omega^{\text{old}} \neq \Lambda_\omega, \quad \forall \omega \in \Omega$ 
18: End:
19: return  $\Omega^* := \bigcup_{\omega \in \Omega} (\Omega_{b(\omega)}^* \cap \Omega_{s(\omega)}^*)$ 

```

that relate the P2P interactions and the operating conditions in the distribution network. To derive these network usage charges, we use DLMPs with the intent to incentivize those P2P transactions that facilitate distribution network operations and penalize those P2P transactions that are unfavorable from the network operation perspective.

We derive the network usage charges using the second-order-cone AC OPF model, [25], that scales well for large networks and makes it possible to derive DLMP components accounting for energy demand, line congestion, nodal voltage, and power losses. Accordingly, the distribution network operations from the utility perspective can be modeled as:

$$\max_{\Xi^{\text{Dist}}} O^{\text{Dist}} := \sum_{b \in \mathcal{B}} [T_b D_b^p (1 - \Gamma_b) - C^u p_b^g] - C^w p_0^g \quad (7a)$$

$$(\lambda_b) : \quad f_{l|s(l)=b}^p - \sum_{l|r(l)=b} (f_l^p - a_l R_l) - p_b^g - g_{n=b}^p + D_b^p + G_b v_b = 0, \quad \forall b \in \mathcal{B}, \quad (7b)$$

$$(\mu_b) : \quad f_{l|s(l)=b}^q - \sum_{l|r(l)=b} (f_l^q - a_l X_l) - q_b^g + D_b^q - B_b v_b = 0, \quad \forall b \in \mathcal{B}, \quad (7c)$$

$$(\eta_l^+) : \quad (f_l^p)^2 + (f_l^q)^2 \leq S_l^2, \quad \forall l \in \mathcal{L}, \quad (7d)$$

$$(\eta_l^-) : \quad (f_l^p - a_l R_l)^2 + (f_l^q - a_l X_l)^2 \leq S_l^2, \quad \forall l \in \mathcal{L}, \quad (7e)$$

$$v_{o(l)} - 2(R_l f_l^p + X_l f_l^q) + a_l (R_l^2 + X_l^2) = v_{r(l)}, \quad \forall l \in \mathcal{L}, \quad (7f)$$

$$\frac{(f_l^p)^2 + (f_l^q)^2}{a_l} \leq v_{o(l)}, \quad \forall l \in \mathcal{L}, \quad (7g)$$

$$\underline{P}_b^g \leq p_b^g \leq \overline{P}_b^g, \quad \forall b \in \mathcal{B}, \quad (7h)$$

$$\underline{Q}_b^g \leq q_b^g \leq \overline{Q}_b^g, \quad \forall b \in \mathcal{B}, \quad (7i)$$

$$\underline{V}_b \leq v_b \leq \overline{V}_b, \quad \forall b \in \mathcal{B}. \quad (7j)$$

where $\Xi^{\text{Dist}} = \{f_l^p, f_l^q, p_b^g, g_n^p, a_l, v_b \geq 0\}$. Objective function O^{Dist} in Eq. (7a) maximizes the profit of the utility given tariff T_b and the amount of load served by the utility $(1 - \Gamma_b)D_b^p$ minus the cost of utility operated generators $C^u p_b^g$ and the cost of purchasing power p_0^g from the wholesale market at price C^w . Note that $p_0^g = 0 - f_0^p$, i.e. all the power purchased

in the wholesale market is injected via the root node of the distribution network. The active and reactive power balance are enforced in Eq. (7b)-(7c). Unlike in the objective function in Eq. (7a), the demand enforced in Eq. (7b)-(7c) accounts for the supply from both the P2P platform and utility, i.e. the resulting DLMPs reflect both components. The apparent power flow limits on the receiving and sending nodes of each line are enforced in Eq. (7d)-(7e). Eq. (7f) relates the line flows and nodal voltages, while Eq. (7g) is the second-order conic constraint that convexifies the original non-convex AC OPF problem, [25]. The active and reactive power output limits on utility generators are enforced in Eq. (7h) and (7i). Eq. (7j) limits nodal voltage magnitudes.

Given the AC OPF formulation in Eq. (7), the DLMPs can be computed as follows, [21]:

$$\lambda_{o(l)} = A_1 \lambda_{r(l)} + A_2 \mu_{o(l)} + A_3 \mu_{r(l)} + A_4 \eta_{o(l)}^+ + A_5 \eta_{o(l)}^-, \quad (8)$$

where parameters A_1, \dots, A_5 are computed based on the optimal OPF solution, as described in Appendix. The DLMPs obtained from Eq. (8) internalizes the effects of binding constraints in Eq. (7b)-(7e) and can be interpreted in terms of distribution line losses, power flow limits and nodal voltage limits, [21]. Given the DLMPs in Eq. (8), we compute the network usage charge for trade ω between buyer $b(\omega)$ and seller $s(\omega)$ as follows:

$$c_\omega^n = (\lambda_{b(\omega)} - \lambda_{s(\omega)})/2, \quad \forall \omega \in \Omega, \quad (9)$$

where the factor of 2 equally splits the network usage charge between the seller and buyer. The equal allocation of the network usage charge is motivated by the assumption that the seller and buyer equally benefit from the transaction and using the distribution network. Given the value of c_ω^n for trade ω the buyer pays $\rho_\omega + c_\omega^n$ and the seller receives the payment of $\rho_\omega - c_\omega^n$. Hence, the total network usage charges collected by the utility can be computed as:

$$NUC(c_\omega^n, p_\omega) := \sum_{\omega \in \Omega^*} 2c_\omega^n p_\omega, \quad (10)$$

where $\sum_{\omega \in \Omega^*} p_\omega = \sum_{n \in \mathcal{N}^b} D_n^p \Gamma_n = \sum_{n \in \mathcal{N}^s} g_n^p$. Note that $NUC(c_\omega^n, p_\omega)$ in Eq. (10) is the second term in Eq. (2).

C. Coordination between the P2P platform and utility

Given the network usage charges, the P2P platform and utility operations can be coordinated to comply with distribution network limits. However, this coordination varies for the system- and peer-centric configurations. Fig. 3 illustrates the coordination for each configuration as further detailed below.

1) *System-centric configuration*: Under the system-centric P2P configuration, the integration between the P2P platform and utility operations can be achieved by co-optimizing the P2P- and utility-end decisions. This co-optimization is shown in Fig. 3(a) and is similar to a pool market design and, therefore, imposes similar requirements on the data that peers need to share with the P2P platform (e.g. consumption and production levels, characteristics of cost and utility functions, among other preferences). Thus, the P2P platform first collects this information from peers. Second, given the collected information, the co-optimization of the P2P transaction and utility-operated distribution assets matches the peers and dispatches

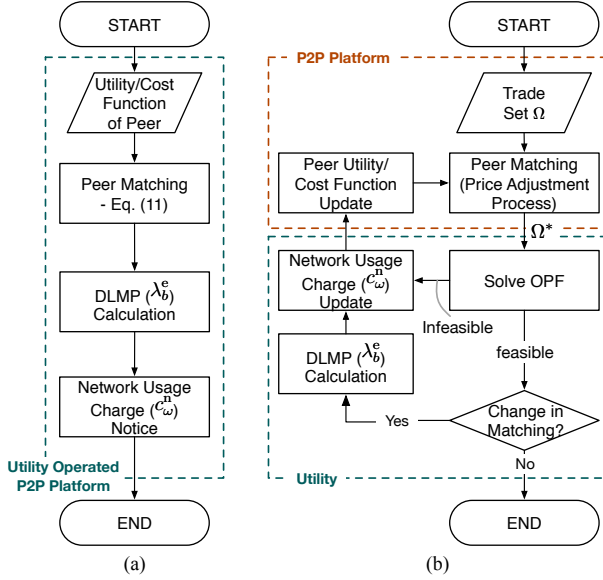


Fig. 3: Coordination between the proposed P2P platform and utility operations using the network usage charges for the (a) system-centric configuration and (b) peer-centric configuration. The dashed boxes delineate P2P- and utility-end procedures.

them to maximize the social welfare and meet distribution network constraints. This co-optimization is formulated as:

$$\max O^{\text{P2P}} + O^{\text{Dist}} \quad (11a)$$

$$\text{Eq. (4b)–(4f)} \quad \text{P2P constraints} \quad (11b)$$

$$\text{Eq. (7b)–(7j)} \quad \text{Network constraints} \quad (11c)$$

Third, once the co-optimization in Eq. (11) is solved, the DLMPs can be computed as in Eq. (8). Finally, given the DLMPs, the P2P platform computes the network usage charges as in Eq. (9), and settles the transactions among the peers.

2) *Peer-centric configuration*: Since the peer-centric coordination assumes that the P2P platform and the utility are operated separately, the coordination is achieved under the iterative procedure displayed in Fig. 3(b). First, the P2P platform generates set of potential trades Ω . Second, the P2P platform matches the peers, i.e. it computes set of selected trades Ω^* and the corresponding price for each trade ρ_ω using Algorithm 1. Next, the utility solves an OPF problem in Eq. (7) given the nodal injections for trades in set Ω^* . Since the trades in set Ω^* are myopic to network limits, solving Eq. (7) may lead to a suboptimal or infeasible solution. To avoid such outcomes, small penalty ϵ is imposed, if the OPF is infeasible, and the network usage charges are computed as:

$$c_\omega^n = \begin{cases} (\lambda_{b(\omega)} - \lambda_{s(\omega)})/2, & \forall \omega \in \Omega^*, \text{ if OPF = feasible} \\ \epsilon, & \forall \omega \in \Omega^*, \text{ if OPF = infeasible} \end{cases} \quad (12)$$

Given the updated value of c_ω^n and trade price ρ_ω , the cost and utility functions of peers in Eq. (6) is updated as follows:

$$\Omega_n^* = \begin{cases} \arg \max_{\Omega_n} \{ \sum_{\omega \in \Omega_n} (\rho_\omega^s - c_\omega^n) p_\omega - C_n(g_n^P) \}, & \forall n \in \mathcal{N}^s \\ \arg \max_{\Omega_n} \{ U_n(d_n^P) - \sum_{\omega \in \Omega_n} (\rho_\omega^b + c_\omega^n) p_\omega \}, & \forall n \in \mathcal{N}^b \end{cases} \quad (13)$$

With the updated cost and utility functions, the iterative procedure in Fig. 3(b) continues until the stable peer match is found. Relative to the system-centric configuration, the iterative procedure allows for accommodating the negotiation process among the peers and prevents from sharing the information about individual peers with the utility.

IV. CASE STUDY

The case study uses the 15-bus distribution system from [21] and the realistic, urban-scale 141-bus distribution feeder from [26]. All models are implemented using the Julia JuMP package and the code and input data are available in [27].

A. 15-bus distribution test system

The distribution system illustrated in Fig. 4 has two producers located at node 1 and 12 with the installed capacity of 2MW and 0.4MW and the incremental cost of \$50/MWh and \$10/MWh, respectively. The total load in the system is 1.63 MW. We select $\Gamma_b = 100\%$, $\forall b \in \mathcal{B}$, i.e. the utility does not supply electricity and only operates the distribution network. Fig. 5 compares the P2P interactions under the system- and peer-centric configurations. While the two producing peers sell roughly the same capacity under both configurations, the sold power capacity is differently allocated among consumers. The peer-centric configuration tends to favor transactions among neighboring buses, i.e. producer at node 1 sells exclusively to the nodes 2 and 13 that are directly adjacent to it. On the other hand, the system-centric configuration results in a more diverse set of the P2P interactions that allows the transactions among electrically remote nodes.

As a result of this different trade allocation, the two P2P configurations lead to different utilizations of the distribution network and, therefore, in different network usage charges. Fig. 6 compares line loading and nodal voltage magnitudes under the two configurations. Since the peer-centric configuration favors transactions among neighboring nodes, it does not fully utilize line capacity and incur lower network usage charges for the peers as shown in Fig. 5. As a result, the peer-centric configuration does not maximize the social welfare of the entire distribution network. On the other hand, the welfare maximum is achieved under the system-centric configuration, where the P2P transactions are explicitly co-optimized with distribution network operations, which leads to a higher utilization of line capacity (Fig. 6) and greater network usage charges (Fig. 5). These differences in utilization of the distribution network lead to different network usage charges and achieve different levels of social welfare as compared in Table I. Accordingly, the system-centric configuration results in a greater revenue of the utility from the network usage charges, while the peer-centric formulation ensures the least-cost electricity supply.

TABLE I. PEER PAYMENTS AND NETWORK USAGE CHARGES

| Configuration | Payments of consumers, $\sum_{\omega} (\rho_\omega + c_\omega^n) p_\omega$ | Revenues of producers, $\sum_{\omega} (\rho_\omega - c_\omega^n) p_\omega$ | NUC, $\sum_{\omega} 2c_\omega^n p_\omega$ | Cost of generation, $\sum_{\omega} C_n(g_n^P)$ |
|----------------|--|--|---|--|
| System-centric | \$88.20 | \$78.17 | \$10.03 | \$70.61 |
| Peer-centric | \$79.46 | \$79.01 | \$0.45 | \$71.80 |

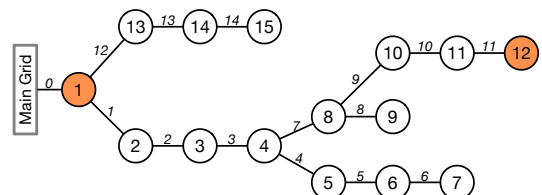


Fig. 4: 15-bus radial distribution system from [21] with nodal indices in circles. Italic numbers above edges represent line indices. Orange nodes represent producing peers.

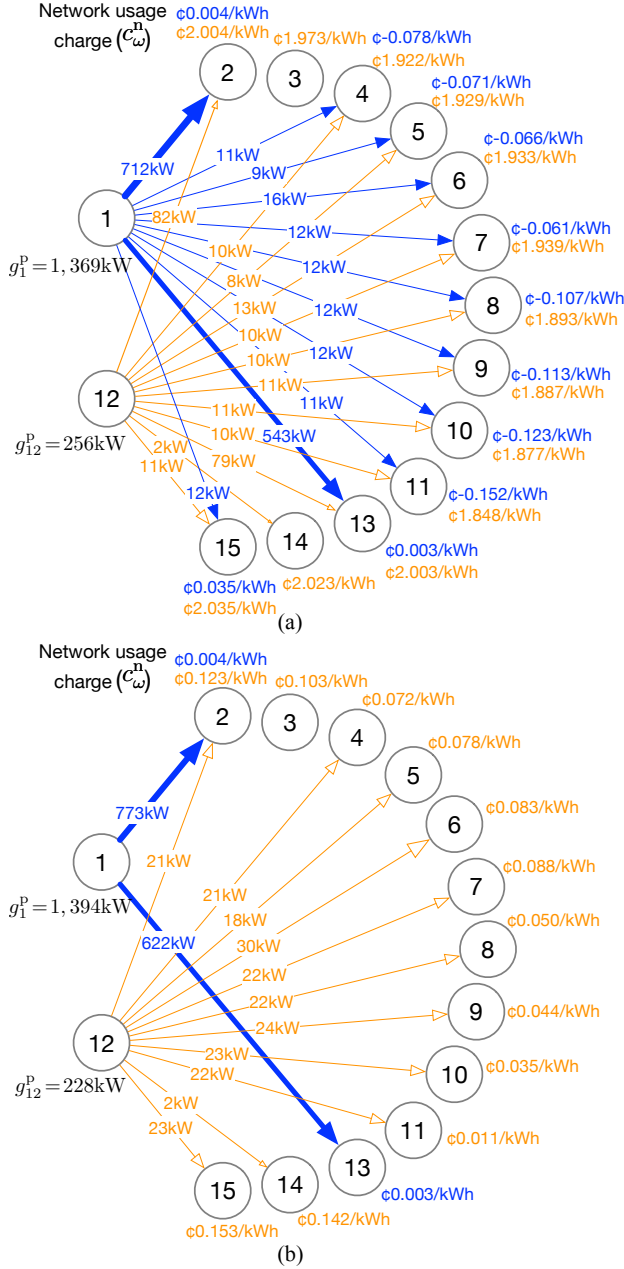


Fig. 5: P2P transactions in 15-bus distribution system under the (a) system-centric and (b) peer-centric configurations. Blue and orange colors represent the trades by producing peers 1 and 12. The network usage charge c_{ω}^n is given next to each consuming peers $b(\omega)$.

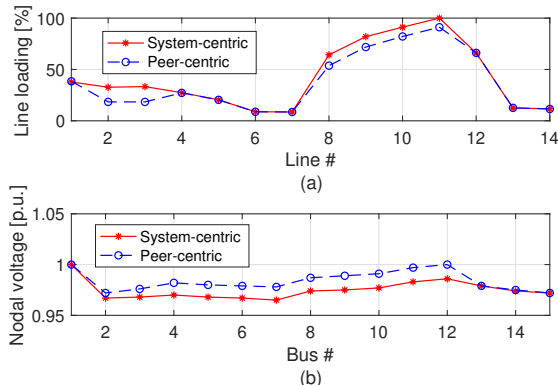


Fig. 6: (a) Distribution line loading (in % relative to S_l) and (b) nodal voltage magnitudes under the system- and peer-centric configurations.

B. 141-bus urban-scale distribution feeder

We add 9 DERs with parameters given in Table II to the 141-bus distribution system from [26], which has the total load of 11.98MW. Different penetration levels of P2P transactions are simulated by varying parameter Γ_b between 0 and 0.6, while assuming that the utility must operate the distribution network and supply the residual demand.

Fig. 7 compares the line loading and voltage magnitudes under the two P2P configurations. As the P2P penetration level increases in both cases, the line loading and its variance across lines monotonically reduce. This reduction is mainly achieved due to the fact that the P2P interactions offset centralized electricity production by local power injections. Similarly, local power injections improve voltage profile across the distribution network due to the reduction of power losses. As a result, the P2P interactions under both configurations lead to sizable reductions in the magnitude and volatility of DLMPs as the P2P penetration level increases, as shown in Fig. 8. The difference in DLMPs under the system- and peer-centric configurations merely exists and further reduces as the P2P platform penetration level increases.

Table III compares average network usage charge $\mathbb{E}(c_{\omega}^n) = \sum_{\omega \in \Omega^*} c_{\omega}^n p_{\omega} / \sum_{\omega \in \Omega^*} p_{\omega}$ of the system- and peer-centric configurations with different P2P platform participation levels Γ_b and corresponding P2P supplied demand $\sum_{b \in \mathcal{B}} \Gamma_b D_b^p$. The system-centric yields higher network usage charges, because it tends to spread the use of P2P resources across the entire distribution network, which maximizes the global welfare. On the other hand, the peer-centric configuration results in lower

TABLE II. LOCATION, INCREMENTAL COST AND CAPACITY OF DGs

| Peer | 1 | 30 | 40 | 50 | 60 | 70 | 80 | 101 | 121 |
|--------------------------|----|----|----|----|----|----|----|-----|-----|
| Incremental Cost, \$/MWh | 20 | 10 | 12 | 11 | 15 | 10 | 17 | 10 | 13 |
| Capacity, MW | 2 | 2 | 2 | 2 | 2 | 2 | 2 | 2 | 2 |

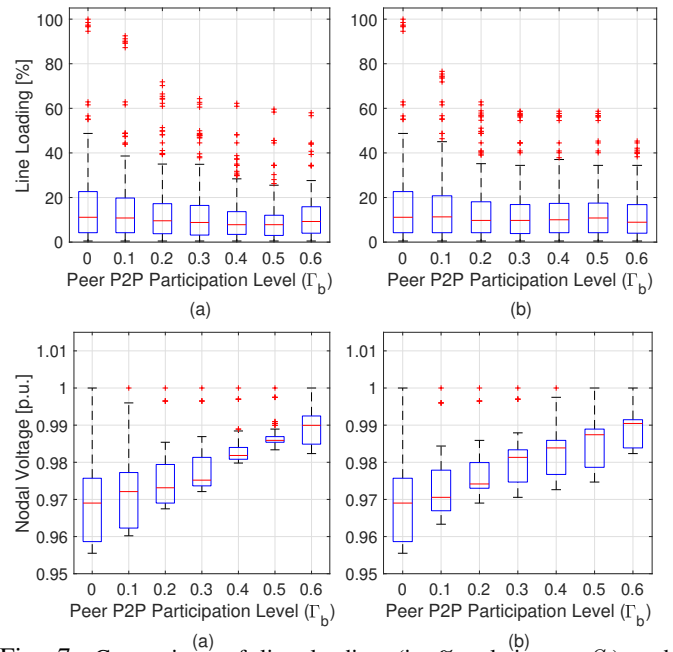


Fig. 7: Comparison of line loading (in % relative to S_l) and voltage magnitudes under the (a) system-centric and (b) peer-centric configurations. The red line within the blue box represents the median value, the bottom and top edges of the box represent the first and third quartiles and the outliers are plotted outside the box in red.

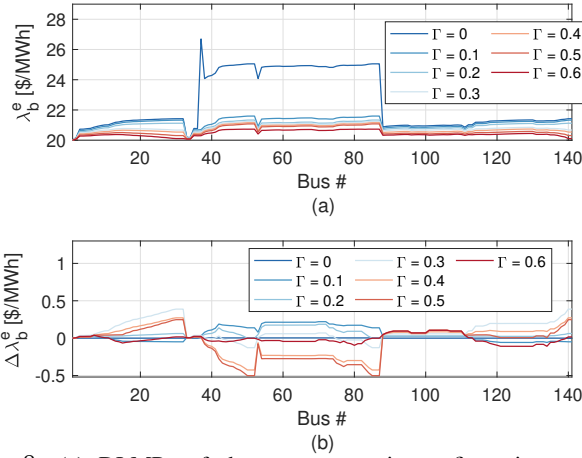


Fig. 8: (a) DLMPs of the system-centric configuration and (b) the difference of DLMPs between the system- and peer-centric configurations ($\Delta\lambda_b = \lambda_b^{\text{SC}} - \lambda_b^{\text{PC}}$) with $\Gamma_b = \Gamma$.

TABLE III. AVERAGE NETWORK USAGE CHARGES

| P2P supplied Demand | Γ_b | 0 | 0.1 | 0.2 | 0.3 | 0.4 | 0.5 | 0.6 |
|--|----------------------------------|---|-------|-------|-------|-------|-------|------|
| | $\sum_b \Gamma_b D_b^{\text{P}}$ | 0 | 1.20 | 2.40 | 3.59 | 4.79 | 5.99 | 7.19 |
| $\mathbb{E}(c_{\omega}^{\text{n}})$, \$/MWh | System | 0 | 0.65 | 0.84 | 0.84 | 0.93 | 0.94 | 0.93 |
| | Peer | 0 | -0.09 | -0.07 | -0.03 | -0.03 | -0.02 | 0.03 |

and, even negative in some cases, network usage charges, because it favors network-friendly P2P trades without accounting for the welfare-maximization.

V. CONCLUSION

This paper describes a new distribution grid architecture with a P2P platform enabling trades among small-scale DERs. The proposed P2P platform can internalize both of the system- and peer-centric matching processes. The system-centric configuration achieves a centralized peer matching in a welfare-maximizing manner and the peer-centric configuration allows peers to reflect their preferences and match in a decentralized way. For both configurations, we use DLMPs to coordinate the distribution system operation and the P2P energy trading and to design network usage charges that peers pay for using the distribution network operated by the utility. Our simulations analyze techno-economic performance of the P2P platform from the perspective of the utility and peers.

REFERENCES

- [1] Utility Dive, "Seattle City Council approves electricity rate hike," 2018. [Online]. Available: <https://goo.gl/A2DV9P>
- [2] PricewaterhouseCoopers (PwC), "Energy transformation: The impact on the power sector business model," 2013.
- [3] Y. Parag and B. K. Sovacool, "Electricity market design for the prosumer era," *Nature Energy*, vol. 1, March 2016.
- [4] S. Burger *et al.*, "A review of the value of aggregators in electricity systems," *Renew. and Sust. En. Rev.*, vol. 77, pp. 395 – 405, 2017.
- [5] V. Demary, "Competition in the sharing economy," Cologne Institute for Economic Research, IW policy paper, Tech. Rep. 19/2015, 2015.
- [6] P. Joskow, "Why do we need electricity retailers or can you get it cheaper wholesale?" 2000. [Online]. Available: <https://goo.gl/HbMZgo>
- [7] I. Perez-Arriaga, J. Jenkins, and C. Batlle, "A regulatory framework for an evolving electricity sector: Highlights of the mit utility of the future study," *Econ. of En. & Env. Policy*, vol. 6, no. 1, 2017.
- [8] T. Morstyn *et al.*, "Bilateral contract networks for peer-to-peer energy trading," *IEEE Trans. Smart Grid*, vol. 10, no. 2, pp. 2026–2035, 2019.
- [9] T. Morstyn, N. Farrell, S. J. Darby, and M. D. McCulloch, "Using peer-to-peer energy-trading platforms to incentivize prosumers to form federated power plants," *Nature Energy*, vol. 3, no. 2, p. 94, 2018.
- [10] T. Morstyn and M. D. McCulloch, "Multi-class energy management for peer-to-peer energy trading driven by prosumer preferences," *IEEE Transactions on Power Systems*, early access, 2018.

- [11] M. Ostrovsky, "Stability in supply chain networks," *Harvard University Economics Working Paper*, vol. 98, pp. 897–923, 05 2008.
- [12] S. Park *et al.*, "Contribution-based energy-trading mechanism in microgrids for future smart grid: A game theoretic approach," *IEEE Trans. on Industrial Electronics*, vol. 63, no. 7, pp. 4255–4265, 2016.
- [13] W. Tushar *et al.*, "Transforming energy networks via peer to peer energy trading: Potential of game theoretic approaches," 2018. [Online]. Available: <https://arxiv.org/abs/1804.00962>
- [14] H. Ahn *et al.*, "Distributed coordination for optimal energy generation and distribution in cyber-physical energy networks," *IEEE Transactions on Cybernetics*, vol. 48, no. 3, pp. 941–954, 2018.
- [15] T. Baroche *et al.*, "Exogenous approach to grid cost allocation in peer-to-peer electricity markets," *arXiv preprint arXiv:1803.02159*, 2018.
- [16] E. Münsing *et al.*, "Blockchains for decentralized optimization of energy resources in microgrid networks," in *IEEE CCTA*, 2017, pp. 2064–2071.
- [17] S. Wang, A. F. Taha, and J. Wang, "Blockchain-assisted crowdsourced energy systems," in *IEEE Pwr & En. Soc. Gen. Meet.*, 2018, pp. 1–5.
- [18] S. Wang *et al.*, "Energy crowdsourcing and peer-to-peer energy trading in blockchain-enabled smart grids," *arXiv:1901.02390*, 2019.
- [19] E. Sorin, L. Bobo, and P. Pinson, "Consensus-based approach to peer-to-peer electricity markets with product differentiation," *IEEE Transactions on Power Systems*, vol. 34, no. 2, pp. 994–1004, 2019.
- [20] J. Guerrero, A. C. Chapman, and G. Verbić, "Decentralized p2p energy trading under network constraints in a low-voltage network," *IEEE Transactions on Smart Grid*, early access, 2018.
- [21] A. Papavasiliou, "Analysis of distribution locational marginal prices," *IEEE Transactions on Smart Grid*, vol. 9, no. 5, pp. 4872–4882, 2018.
- [22] M. Caramanis *et al.*, "Co-optimization of power and reserves in t&d power markets," *Proc. of IEEE*, vol. 104, no. 4, pp. 807–836, 2016.
- [23] J. Blasch, M. Filippini, and N. Kumar, "Boundedly rational consumers, energy and investment literacy, and the display of information on household appliances," *Res. and En. Econ.*, 2017.
- [24] A. Cavoukian, J. Polonetsky, and C. Wolf, "Smartprivacy for the smart grid: embedding privacy into the design of electricity conservation," *Identity in the Inf. Soc.*, vol. 3, no. 2, pp. 275–294, Aug 2010.
- [25] M. Farivar and S. H. Low, "Branch flow model: Relaxations and convexification - part i," *IEEE Trans. Pwr. Syst.*, vol. 28, no. 3, 2013.
- [26] H. Khodr *et al.*, "Maximum savings approach for location and sizing of capacitors in distribution systems," *El. Pwr. Syst. Res.*, vol. 78, no. 7, pp. 1192–1203, 2008.
- [27] J. Kim and Y. Dvorkin, "Code supplement," 2018. [Online]. Available: <https://github.com/jipkim/P2P>

APPENDIX

As derived in [21], the DLMPs are computed for the origin node $o(l)$ of line l as follows:

$$\lambda_{o(l)} = A_1 \lambda_{r(l)} + A_2 \mu_{o(l)} + A_3 \mu_{r(l)} + A_4 \eta_{o(l)}^+ + A_5 \eta_{o(l)}^- \quad (14a)$$

where $\mu_{o(l)}$, $\mu_{r(l)}$, $\eta_{o(l)}^+$ and $\eta_{o(l)}^-$ are the dual variables of the optimization in Eq. (7) and parameters A_1, A_2, A_3, A_4, A_5 denote the following functional expressions:

$$A_1 = \frac{((f_l^{\text{P}})^2 + (f_l^{\text{Q}})^2)X_l + a_l f_l^{\text{Q}}(R_l^2 - X_l^2) - 2a_l f_l^{\text{P}} R_l X_l}{((f_l^{\text{P}})^2 + (f_l^{\text{Q}})^2)X_l - a_l f_l^{\text{Q}}(R_l^2 + X_l^2)} \quad (14b)$$

$$A_2 = \frac{((f_l^{\text{P}})^2 + (f_l^{\text{Q}})^2)R_l - a_l f_l^{\text{P}}(R_l^2 + X_l^2)}{((f_l^{\text{P}})^2 + (f_l^{\text{Q}})^2)X_l - a_l f_l^{\text{Q}}(R_l^2 + X_l^2)} \quad (14c)$$

$$A_3 = \frac{-((f_l^{\text{P}})^2 + (f_l^{\text{Q}})^2)R_l + a_l f_l^{\text{P}}(R_l^2 - X_l^2) + 2a_l f_l^{\text{Q}} R_l X_l}{((f_l^{\text{P}})^2 + (f_l^{\text{Q}})^2)X_l - a_l f_l^{\text{Q}}(R_l^2 + X_l^2)} \quad (14d)$$

$$A_4 = \frac{2((f_l^{\text{Q}})^3 R_l - (f_l^{\text{P}})^3 X_l) + 2f_l^{\text{P}} f_l^{\text{Q}}(f_l^{\text{P}} R_l - f_l^{\text{Q}} X_l)}{((f_l^{\text{P}})^2 + (f_l^{\text{Q}})^2)X_l - a_l f_l^{\text{Q}}(R_l^2 + X_l^2)} \quad (14e)$$

$$A_5 = \frac{2((f_l^{\text{Q}})^3 R_l - 2(f_l^{\text{P}})^3 X_l) + 2f_l^{\text{P}} f_l^{\text{Q}}(f_l^{\text{P}} R_l - f_l^{\text{Q}} X_l)}{((f_l^{\text{P}})^2 + (f_l^{\text{Q}})^2)X_l - a_l f_l^{\text{Q}}(R_l^2 + X_l^2)} + \frac{2a_l^2(f_l^{\text{Q}} R_l^3 - f_l^{\text{P}} X_l^3) - 4a_l f_l^{\text{P}} f_l^{\text{Q}}(R_l^2 - X_l^2)}{((f_l^{\text{P}})^2 + (f_l^{\text{Q}})^2)X_l - a_l f_l^{\text{Q}}(R_l^2 + X_l^2)} + \frac{4a_l R_l X_l((f_l^{\text{P}})^2 - (f_l^{\text{Q}})^2)}{((f_l^{\text{P}})^2 + (f_l^{\text{Q}})^2)X_l - a_l f_l^{\text{Q}}(R_l^2 + X_l^2)} + \frac{-2a_l^2 R_l X_l(f_l^{\text{P}} R_l - f_l^{\text{Q}} X_l)}{((f_l^{\text{P}})^2 + (f_l^{\text{Q}})^2)X_l - a_l f_l^{\text{Q}}(R_l^2 + X_l^2)} \quad (14f)$$